Electronic Supplementary Material (ESI) for Nanoscale.

Supplementary Information

Prediction of Novel Two-Dimensional Dirac Nodal Line Semimetals in Al_2B_2 and AlB_4 Monolayers

Saeid Abedi,[†] Esmaeil Taghizadeh Sisakht,[*,†] S. Javad Hashemifar,[†] Nima Ghafari Cherati,[†] Ismaeil Abdolhosseini Sarsari,[†] and Francois M. Peeters[‡]

[†]*Department of Physics, Isfahan University of Technology, Isfahan, 84156-83111, Iran.*

[‡]*Department of Physics, University of Antwerp, Groenenborgerlaan 171, B-2020 Antwerpen, Belgium.*

E-mail: taghizadeh.sisakht@gmail.com

■ Continuum model for Al_2B_2 configuration around K point.

Table S1: Symmetrized matrices for the invariant expansion of the diagonal blocks $\mathcal{H}_{ii}$ for the point group D_{3h}.

Block	Representations	Symmetrized matrices		Tensor components	
$\mathcal{H}_{11}$	$\Gamma_6 \otimes \Gamma_6^*$	$\Gamma_1:$	$\mathbb{1}$	$\Gamma_1:$	$\mathbb{1};\ k_x^2 + k_y^2$
	$= \Gamma_1 + \Gamma_2 + \Gamma_6$	$\Gamma_2:$	σ_z	$\Gamma_2:$	$-$
		$\Gamma_6:$	σ_x, σ_y	$\Gamma_6:$	$(k_x, k_y); (k_y^2 - k_x^2, 2k_xk_y)$
$\mathcal{H}_{22}$	$\Gamma_4 \otimes \Gamma_4^*$	$\Gamma_1:$	$\mathbb{1}$	$\Gamma_1:$	$\mathbb{1};\ k_x^2 + k_y^2$
	$= \Gamma_1$				

The diagonalization of parameter-dependent Hamiltonian (1) of the main text results in the three-band energy spectra

$$E_{1,2}(k_x, k_y) = E_0 + A({k_x}^2 + {k_y}^2) \pm \sqrt{B^2({k_x}^2 + {k_y}^2) + C^2({k_x}^2 + {k_y}^2)^2 - 2BC({k_x}^3 - 3k_x{k_y}^2)}, \quad \text{(S1)}$$

$$E_3(k_x, k_y) = E_0' + A'({k_x}^2 + {k_y}^2). \quad \text{(S2)}$$

The fitted parameters are $E_0 = 1.19$ eV, $A = -113.16$ eVÅ^2, $B = 8.78$ eVÅ, $C = 132.10$ eVÅ^2, $E_0' = -0.56$ eV, $A' = 66.33$ eVÅ^2. The fitted bands are shown in Fig. S1. A comparison between the DFT bands and the bands from our continuous model shows that although continuum energy bands do not fit well by moving away from K point, they reproduce well the band dispersions near the K point and thus the distribution of NL1.

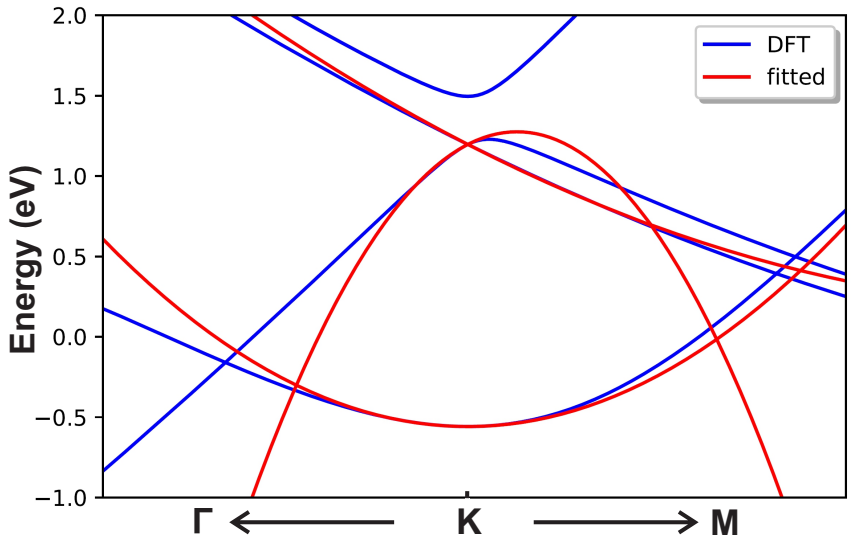

Figure S1: Comparison between DFT bands and the bands from the continuum model near the K point of Al_2B_2.

■ Continuum model for Al_2B_2 configuration around Γ point.

Table S2: Symmetrized matrices for the invariant expansion of the diagonal blocks $\mathcal{H}_{ii}$ for the point group D_{6h}.

Block	Representations	Symmetrized matrices	Tensor components
$\mathcal{H}_{11}$	$\Gamma_6^+ \otimes \Gamma_6^{+*}$	Γ_1^+ : $\mathbb{1}$	Γ_1^+ : $\mathbb{1};\ k_x^2 + k_y^2$
	$= \Gamma_1^+ + \Gamma_2^+ + \Gamma_6^+$	Γ_2^+ : σ_z	Γ_2^+ : $-$
		Γ_6^+ : σ_x, σ_y	Γ_6^+ : $(k_y^2 - k_x^2, 2k_xk_y);\ (k_x^4 - 6k_x^2k_y^2 + k_y^4, 4k_xk_y^3 + 4k_x^3k_y)$
$\mathcal{H}_{22}$	$\Gamma_2^- \otimes \Gamma_2^{-*}$	Γ_1^+ : $\mathbb{1}$	Γ_1^+ : $\mathbb{1};\ k_x^2 + k_y^2$
	$= \Gamma_1^+$		

Energy bands as obtained from the continuum model:

$$E_{1,2}(k_x, k_y) = E_0 + A({k_x}^2 + {k_y}^2) \pm \sqrt{B^2({k_x}^2 + {k_y}^2)^2 + C^2({k_x}^2 + {k_y}^2)^4 - 2BC({k_x}^6 - 15{k_x}^4{k_y}^2 + 15k_x^2k_y^4 - k_y^6)}, \tag{S3}$$

$$E_3(k_x, k_y) = E_0' + A'({k_x}^2 + {k_y}^2). \tag{S4}$$

The fitted parameters are $E_0 = -0.37$ eV, $A = -43.88$ eVÅ^2, $B = 11.10$ eVÅ^2,$C = 100.17$ eVÅ^4, $E_0' = -2.85$ eV, $A' = 12.36$ eVÅ^2. Using the fitted values we have shown in Fig. S2 a comparison between DFT bands and the bands from our continuum model.

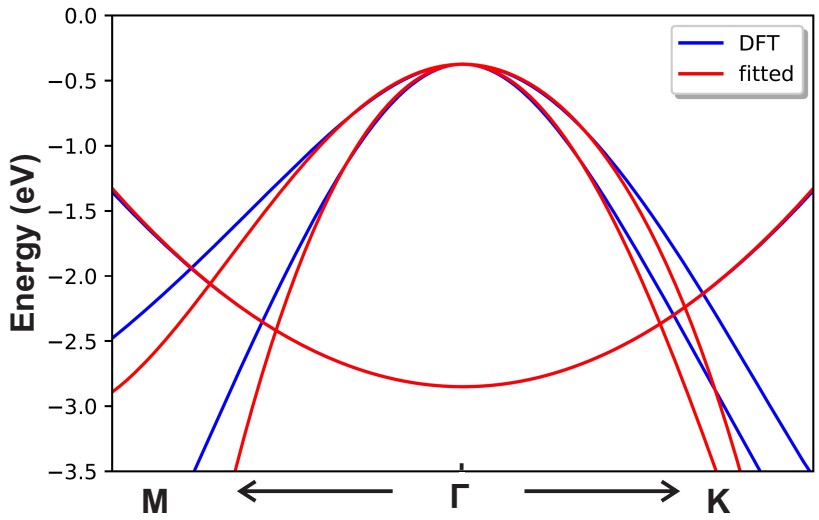

Figure S2: Comparison between DFT bands and the bands from the continuum model near the Γ point of Al_2B_2.

■ Continuum model for AlB_4 around the Γ point.

Table S3: Symmetrized matrices for the invariant expansion of the diagonal blocks $\mathcal{H}_{ii}$ for the point group D_{6h}.

Block	Representations	Symmetrized matrices		Tensor components	
$\mathcal{H}_{11}$	$\Gamma_6^- \otimes \Gamma_6^{-*}$	$\Gamma_1^+:$	$\mathbb{1}$	$\Gamma_1^+:$	$\mathbb{1};\ k_x^2+k_y^2$
	$=\Gamma_1^+ + \Gamma_2^+ + \Gamma_6^+$	$\Gamma_2^+:$	σ_z	$\Gamma_2^+:$	$-$
		$\Gamma_6^+:$	σ_x, σ_y	$\Gamma_6^+:$	$(k_y^2-k_x^2, 2k_xk_y);\ (k_x^4-6k_x^2k_y^2+k_y^4, 4k_xk_y^3+4k_x^3k_y)$
$\mathcal{H}_{22}$	$\Gamma_6^+ \otimes \Gamma_6^{+*}$	$\Gamma_1^+:$	$\mathbb{1}$	$\Gamma_1^+:$	$\mathbb{1};\ k_x^2+k_y^2$
	$=\Gamma_1^+ + \Gamma_2^+ + \Gamma_6^+$	$\Gamma_2^+:$	σ_z	$\Gamma_2^+:$	$-$
		$\Gamma_6^+:$	σ_x, σ_y	$\Gamma_6^+:$	$(k_y^2-k_x^2, 2k_xk_y);\ (k_x^4-6k_x^2k_y^2+k_y^4, 4k_xk_y^3+4k_x^3k_y)$
$\mathcal{H}_{33}$	$\Gamma_2^- \otimes \Gamma_2^{-*}$	$\Gamma_1^+:$	$\mathbb{1}$	$\Gamma_1^+:$	$\mathbb{1};\ k_x^2+k_y^2$
	$=\Gamma_1^+$				

Energy bands as obtained from the continuum model:

$$E_{1,2}(k_x,k_y) = E_0 + A({k_x}^2+{k_y}^2) \pm \sqrt{B^2({k_x}^2+{k_y}^2)^2 + C^2({k_x}^2+{k_y}^2)^4 - 2BC({k_x}^6 - 15{k_x}^4{k_y}^2 + 15k_x^2k_y^4 - k_y^6)}, \tag{S5}$$

$$E_{3,4}(k_x,k_y) = E_0' + A'({k_x}^2+{k_y}^2) \pm \sqrt{B'^2({k_x}^2+{k_y}^2)^2 + C'^2({k_x}^2+{k_y}^2)^4 - 2B'C'({k_x}^6 - 15{k_x}^4{k_y}^2 + 15k_x^2k_y^4 - k_y^6)}, \tag{S6}$$

$$E_5(k_x,k_y) = E_0'' + A''({k_x}^2+{k_y}^2). \tag{S7}$$

By fitting the parameters with DFT results, we obtain $E_0 = 0.28$ eV, $A = -42.10$ eVÅ^2, $B = 12.55$ eVÅ^2,$C = 74.19$ eVÅ^4, $E_0' = 0.88$ eV, $A' = -36.14$ eVÅ^2, $B' = 8.80$ eVÅ^2,$C' = 58.35$ eVÅ^4, $E_0'' = -2.72$ eV, $A'' = 11.64$ eVÅ^2. The comparison between DFT bands and the bands from the continuum model near the Γ point of AlB_4 is shown in Fig. S3.

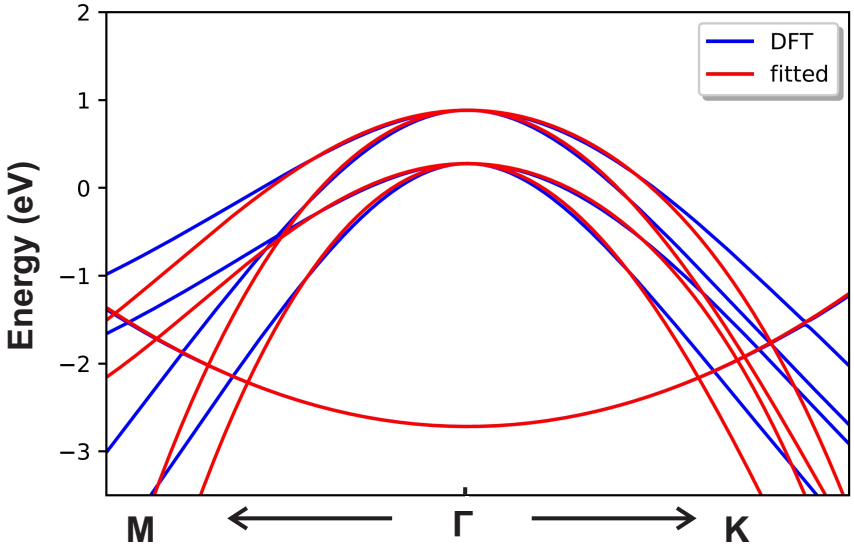

Figure S3: Comparison between DFT bands and the bands from the continuum model near the Γ point of AlB_4.

■ Mirror eigenvalues of electronic bands in Al_2B_2 and AlB_4.

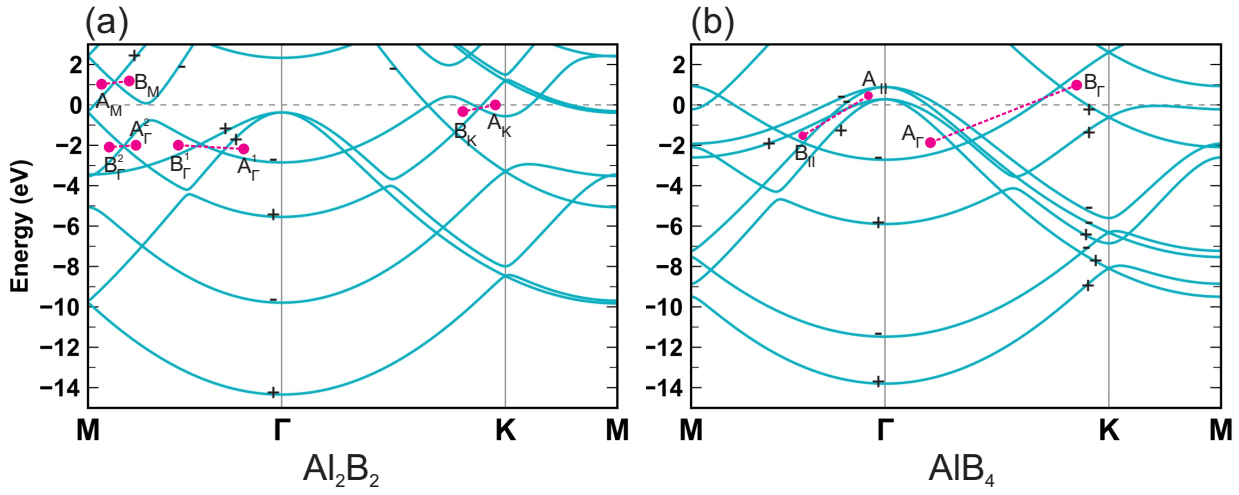

Figure S4: Mirror eigenvalues of selected bands for (a) Al_2B_2 and (b) AlB_4 monolayers. The picked points in tables I and II are also shown by magenta circles.

■ Electronic band structures of Al_2B_2 and AlB_4 with SOC effect.

Both Al_2B_2 and AlB_4 monolayers have spatial inversion (P) and time-reversal (T) symmetry. Therefore, with the inclusion of SOC, the combined symmetry PT ensures that each band is doubly degenerate. In addition, the resulting Kramers pair has opposite M_z eigenvalues $\pm i$ that impose an interaction between energy bands that form mirror-protected NLs, and one expects to observe a tiny gap at nodal points.[1] Figure S5 shows the electronic band structures of Al_2B_2 and AlB_4 monolayers with the SOC effect. It turns out that the SOC strength induces tiny gaps (less than 4 meV) at all crossing nodal points. It is worth mentioning that the SOC induced gaps are more sizable for experimentally realized 2D NLs[2–4] than that of monolayer Al_2B_2 and AlB_4. In comparison, the NLs in these materials are more robust and thus very likely to be observed in future experiments.

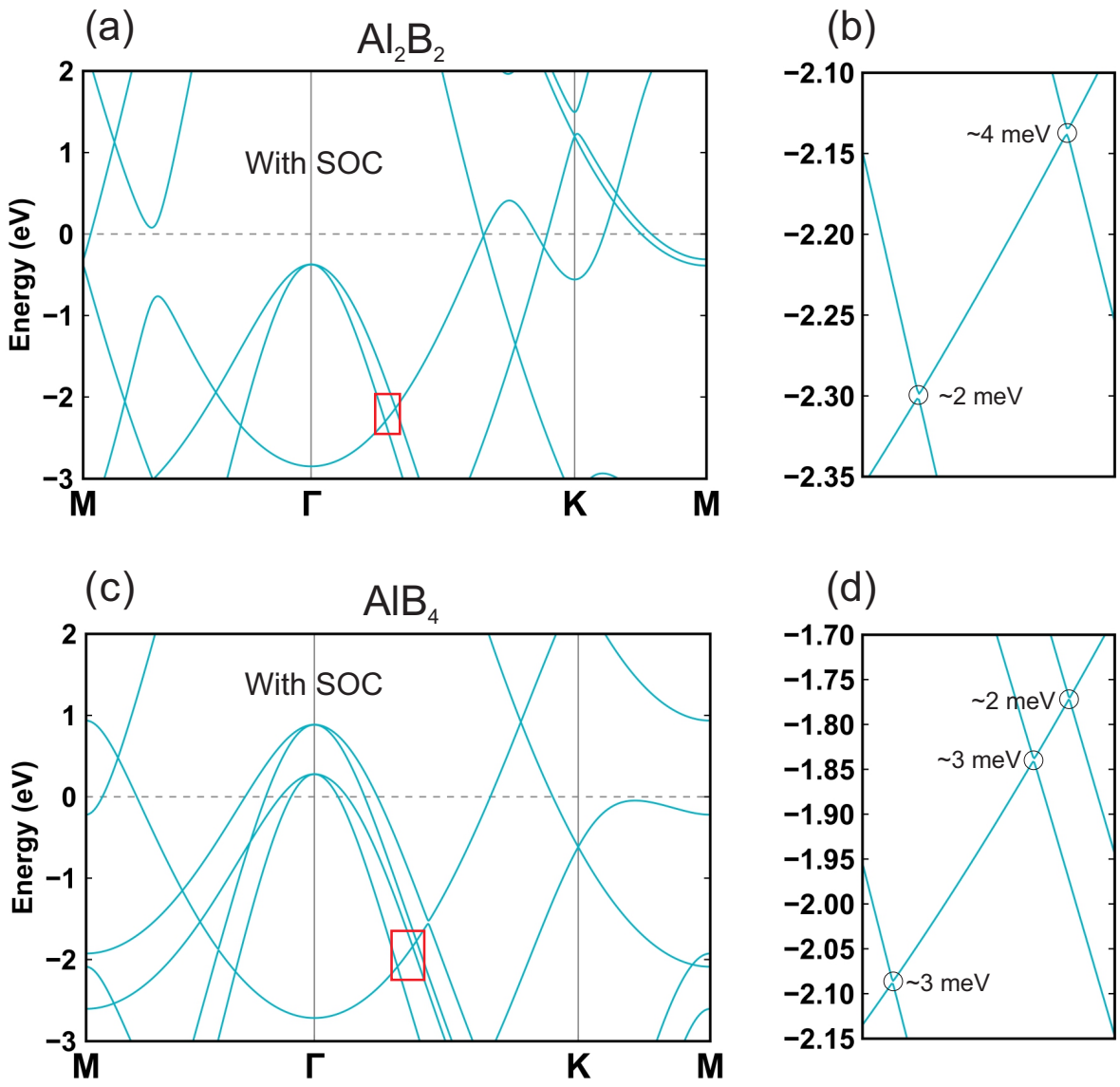

Figure S5: Calculated electronic band structure of (a) Al_2B_2 and (c) AlB_4 with the inclusion of SOC effect. (b) and (d) Zoom-in band structures in the red rectangles in (a) and (c) to clearly show the SOC-induced gaps.

■ Electronic properties of monolayer AlB_2.

The electronic band structure of freestanding monolayer AlB_2 is shown in Fig. S6. Within 2.5 eV of the Fermi level there are several bands which cross and form four $p-$type Dirac cones below (red circles) and a gapless $n-$type Dirac cone above (blue circle) the Fermi surface, respectively. We mark these bands by Greek letters as shown in the figure. Group theory analysis of these energy bands shows that along the Γ-M and K-M symmetry directions

the symmetry groups is C_s which has an out of plane symmetry element. Along these directions β, γ and δ bands belong to the Γ_1 IR which have positive mirror parities. Also, the IR of α and ν bands are Γ_2 with a negative mirror eigenvalue.[5] As a result, within the mentioned energy window one can observe the formation of four Dirac points DP1-DP4 due to the crossing of bands with opposite mirror parities. The remaining Dirac point (DP3) is located at the K point which arises from the boron hexagonal lattice as for the Dirac cones in graphene. Note that due to the absence of in-plane mirror symmetry in monolayer AlB_2, along arbitrary low-symmetry directions X-Γ and X′-K one can see no crossing (see Figs. S7 a and b). Therefore, we do not expect symmetry protected NLs in this structure. The existence of $p-$type Dirac Fermions in this configuration has been confirmed by recent ARPES measurements.[6]

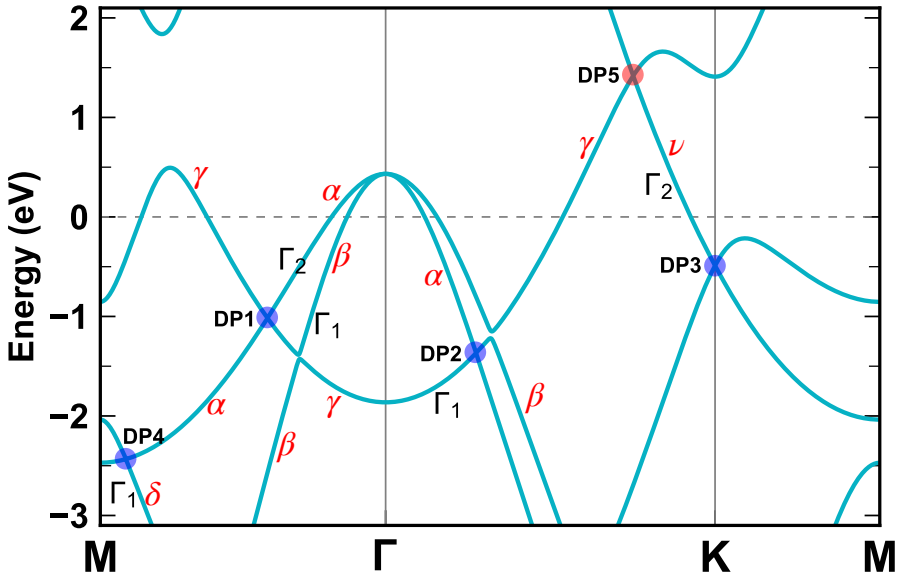

Figure S6: The electronic band structure of monolayer AlB_2 along the high symmetry paths M-Γ-K-M. The $p-$ and $n-$type Dirac cones are shown by red and blue circles, respectively.

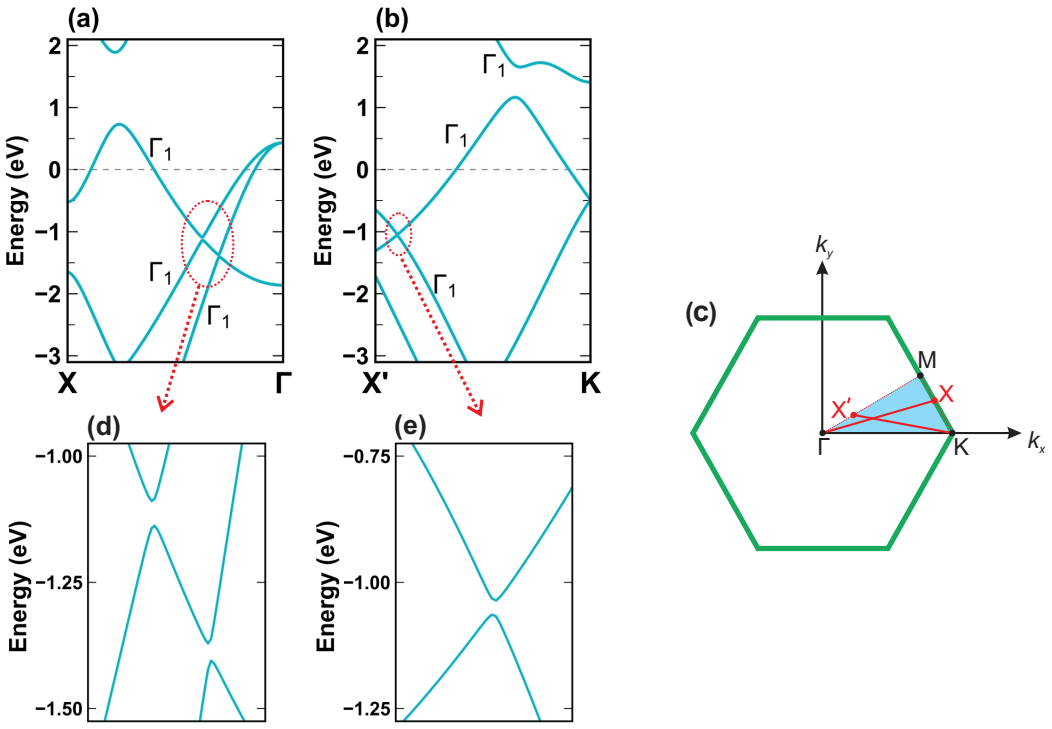

Figure S7: The electronic band structure of monolayer AlB_2 along typical low-symmetry directions (a) X-Γ and (b) X′-K as shown in (c). The zoomed-in band structures indicated by the red ellipses are shown in (d) and (e).

References

(1) Gao, H.; Venderbos, J. W.; Kim, Y.; Rappe, A. M. *Annu. Rev. Mater. Res.* **2019**, *49*, 153–183.

(2) Feng, B. et al. *Nat. Commun.* **2017**, *8*, 1007.

(3) Gao, L.; Sun, J.-T.; Lu, J.-C.; Li, H.; Qian, K.; Zhang, S.; Zhang, Y.-Y.; Qian, T.; Ding, H.; Lin, X.; Du, S.; Gao, H.-J. *Adv. Mater.* **2018**, *30*, 1707055.

(4) Liu, B.; Liu, J.; Miao, G.; Xue, S.; Zhang, S.; Liu, L.; Huang, X.; Zhu, X.; Meng, S.; Guo, J.; Liu, M.; Wang, W. *J. Phys. Chem. Lett.* **2019**, *10*, 1866–1871.

(5) Altmann, S. L.; Herzig, P. *Point-group theory tables*; Claredon Press, Oxford, 1994.

(6) Geng, D. et al. *Phys. Rev. B* **2020**, *101*, 161407.